Optimal Signal Selection for Power System Ambient Mode Estimation Using a Prediction Error Criterion

Vedran S. Perić, *Student Member, IEEE*, Xavier Bombois, and Luigi Vanfretti, *Senior Member, IEEE*

***Abstract*—This paper formulates an optimality criterion for the selection of synchrophasor signals to be used in ambient mode estimators. This criterion, which is associated with each measured signal and each dominant mode, is defined as the asymptotic variance of the corresponding estimated mode damping ratio. The value of the criterion is computed directly from an estimated autoregressive moving average (ARMA) model. Because the online computation of the defined criterion (for each measured signal in the system) may be computationally expensive, a fast pre-selection method for initial signal ranking is formulated. The pre-selection method is used to effectively determine a set of the candidate signals for which the formal criterion is evaluated in a second stage. The methodology is illustrated using synthetic measurements from the KTH Nordic 32 and the IEEE 39-bus test systems.**

***Index Terms*—Mode estimation, mode meter, PMU placement, prediction error, signal selection.**

I. Introduction

THE development of synchrophasor technology has enabled better monitoring of electromechanical oscillations and consequently improved situational awareness of power systems [1]. Oscillations are monitored by continuously estimating parameters of critical system modes (frequencies and damping ratios) that predominantly cause the observed oscillations [2]. The tools that have been developed for this purpose (often referred to as mode estimators) estimate parameters of the critical modes by applying system identification theory and techniques. In recent years numerous system identification approaches have been investigated with the aim to improve the robustness and accuracy of the estimates [2], [3]. Commonly used approaches for mode estimation include: 1) prediction error methods [4], 2) frequency domain decomposition [5] and 3) subspace identification methods [6]. Frequency domain decomposition and subspace methods are computationally efficient and suitable for multi-channel analysis, but provide only limited information about the quality of the estimated model. On the other hand, prediction error methods have a firm mathematical foundation which provides additional insight in the estimation process as well as the uncertainty of the estimated model. These methods use an optimization technique to determine model parameters with the objective to minimize the discrepancy between measured and model responses.

In recent years there has been a trend of increasing the number of PMU installations in power systems, leading to a high degree observability of the system [7]. However, since not all synchrophasor signals contain equal amount of information about the critical mode of interest, it can be shown that only a limited number of carefully selected signals contain sufficient information for accurate mode estimation. Furthermore, concurrent use of large number of signals imposes higher computational complexity that may not be suitable for online applications. This reasoning poses the research question of optimal signal selection for mode estimation. The first attempts to address this question have been presented in [8] and [9]. In [8], a Modal Power Contribution (MPC) is proposed as a signal selection criterion, while in [9], suitable signals are selected based on the geometry of the signals' power spectra. In the more recent papers [10] and [11], two level algorithms for mode estimation have been proposed. In these papers, signals contribute to the final mode estimation according to their weighting factors that represent signals' quality. In [10], the weighting factor is defined as a Fourier Transform magnitude at the critical mode's frequency, whereas in [11], the mode energy is used instead. The means for quantifying the signals' relevance for mode estimation (either signal selection criteria [8], [9] or weighting factors [10], [11]) have been developed based on heuristics without a formal proof that the selected signals provide the best possible mode estimation.

The problem of optimal signal selection can be also seen as a problem of optimal PMU placement for mode estimation with the question where to install PMUs to obtain the best possible estimation of the critical mode. To the authors' best knowledge, this question has not been formulated, even though optimal PMU placement (for other applications such as state estimation and stability assessment) has been investigated in the literature [12], [13]. In the traditional PMU placement problem formulations, the optimization criterion is mainly defined as a maximum observability. This observability is defined either in terms of its numerical observability or topological observability [13]. However, the methods developed do not provide information about the optimal signals that should be used to obtain accurate mode estimation.

Manuscript received October 14, 2014; revised March 14, 2015 and July 19, 2015; accepted September 02, 2015. Date of publication September 28, 2015; date of current version May 02, 2016. The work of V.S. Perić was supported by European Commission through the iTesla FP7 project. The work of L. Vanfretti was supported by Nordic Energy Research through the STONg2rid project, by European Commission through the iTesla FP7 project, and Statnett SF. Paper no. TPWRS-01415-2014

V. S. Perić is with the KTH Royal Institute of Technology, SE-10044 Stockholm, Sweden (e-mail: vperic@kth.se).

X. Bombois is with Laboratoire Ampère UMR CNRS 5005, Ecole Centrale de Lyon, 69134 Lyon, France (e-mail: xavier.bombois@ec-lyon.fr).

L. Vanfretti is with KTH Royal Institute of Technology, SE-10044 Stockholm, Sweden and Statnett SF, 0423 Oslo, Norway (e-mail: luigiv@kth.se; luigi.vanfretti@statnett.no).

Color versions of one or more of the figures in this paper are available online at http://ieeexplore.ieee.org.

Digital Object Identifier 10.1109/TPWRS.2015.2477490

An estimate of the critical mode's damping ratio can be seen as a realization of a random variable whose variance depends on the signal that is selected as an input to the mode estimator. Therefore, if an unbiased mode estimator is used, *the best signal for mode estimation is the one that provides the smallest variance of the critical mode's damping ratio*. This means that *the variance represents the criterion* for ranking signals according to their quality for mode estimation.

This paper provides a formal algorithm to compute the (asymptotic) variances of the critical parameter estimates for each signal, under the assumption that the signals' power spectra are known in the form of AutoRegressive Moving Average (ARMA) models. The best signals (for mode estimation) are then determined by ranking the signals according to the calculated variances. This algorithm has its foundation in a theorem (presented in Section III-A) that gives a formula for the parameter covariance matrix (and consequently the variances of interest) of an arbitrary model parameterization.

The proposed algorithm has an advantage that it uses only parameters of the ARMA models as an input to the algorithm. This makes the variance computation independent of the method used to determine the ARMA models. In the case of off-line PMU placement (for mode estimation), the ARMA models can be obtained from the existing physical power system model (off-line simulation). On the other hand, in the case of selecting the best from the set of available synchrophasor measurements, any identification method [2]–[6] can be used (on-line operation).

The proposed algorithm represents a formal approach in determining optimal signals for mode estimation; however, in an on-line setting, it may be computationally expensive to run this algorithm for each signal. For this reason, a fast pre-selection method is formulated in order to determine a limited number of signals which are candidates for the optimal signal (first stage). Later, the formal approach (second stage) is applied only on the signals selected in the first stage to determine the optimal ranking of the signals. The proposed methods are applied to synthetic signals from the KTH Nordic 32 and IEEE 39 bus test systems.

The reminder of this paper is organized as follows. Section II provides relevant background and the approach used for optimal signal selection. The algorithm for computation of the covariance matrix of the estimated parameters is introduced in Section III. The pre-selection method is presented in Section IV. Application of the theory and developed techniques is demonstrated in Section V. Conclusions are drawn in Section VI.

II. Background and Approach

A power system's ambient response, which can be observed in measured synchrophasor signals, is a result of random fluctuations of loads in the power system [3]. These random load fluctuations at the aggregated level can be represented by white noise [14]. Assuming linearity of the power system, its model can be represented as a set of transfer functions from each input (load) to the each output (measured synchrophasor signal) as shown in [14]. This leads to a mathematical description of the i-th measured synchrophasor output y_i:

$$y_i(t) = H_{i1}\hat{e}_1(t) + H_{i2}\hat{e}_2(t) + \ldots + H_{1N}\hat{e}_N(t), \quad (1)$$

where H_{ij} is the transfer function from the j-th input to i-th output and $\hat{e}_j$the disturbance associated to the j-th input (modelled as a white noise of variance $\hat{\sigma}_j^2$).

Consequently, the corresponding power spectrum of the signal $y_i(t)$ can be written as:

$$\Phi_{yi}(f) = |H_{i1}|^2\hat{\sigma}_1^2 + |H_{i2}|^2\hat{\sigma}_2^2 + \ldots + |H_{1N}|^2\hat{\sigma}_N^2 = |G_{0i}|^2\sigma_i^2 \quad (2)$$

As shown in (2), this spectrum can also be expressed using one single transfer function G_{0i} that is excited by a white noise with variance σ_i^2. The modes of G_{0i} are equal to the modes of the original system (power system). The transfer function G_{0i} can be assumed to be proper, monic and has a stable inverse.

A parametric (ARMA) model G_{0i} can be deduced from two sources:

1) *From the measured data*. Measured data is used to find the best signals for mode estimation among the set of given measured signals (on-line operation).
2) *From the existing power system model*. The existing model is used to determine the best locations for PMUs (off-line simulation). This is usually referred to as an optimal PMU placement problem. One way of deducing ARMA models from the existing simulation model is to apply a frequency domain fitting procedure as presented in [15]. In this case the frequency domain data are obtained from (2) at an arbitrary number of frequency points. An alternative approach is to perform a time domain system identification using the data synthetized from the model response. It should be noted that a large identification dataset can be generated and used for this purpose, meaning that the estimated ARMA model can be arbitrary close to G_{0i} [16].

The sequel presents how to obtain the ARMA model from measured data using a prediction error method, assuming that the same procedure can be used for PMU placement problem formulation i.e. when the ARMA models are computed using the existing power system model[1]. Since the prediction error method can also be used for the on-line mode tracking (estimation), a mathematical description of the estimation error is provided as well. This estimation error analysis is used later to define the criterion for optimal signal selection.

Using measured data $y_i(t)$ $(t = 1 \ldots N)$, the estimate of true system G_{0i} (denoted by $G_i(\hat{\theta})$) is determined within an ARMA model structure $G_i(\theta)$. The identified parameter vector $\hat{\theta}$ is the one that minimizes the prediction error criterion $(1/N)\sum_{t=1}^{N}\varepsilon^2(t,\theta) = (1/N)\sum_{t=1}^{N}(G_i^{-1}(\theta)y_i(t))^2$. Suppose that the model structure $G_i(\theta)$ is sufficiently rich to describe the true system G_{0i} (i.e. there is a vector of parameters θ_0 for which $G_i(\theta_0) = G_{0i}$), then the estimate $\hat{\theta}$ is a consistent estimate of that true parameter vector θ_0. Moreover, it can be proven that asymptotically the estimate $\hat{\theta}$ is an unbiased estimate of θ_0 and that the estimate $\hat{\theta}$ is normally distributed

[1]Other identification methods can be used for estimation of ARMA models as well [2], [5], [6].

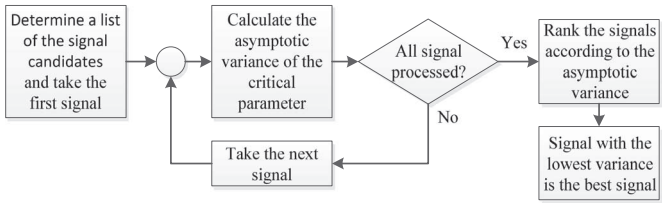

Fig. 1. Global algorithm of optimal signal selection for ambient mode estimation.

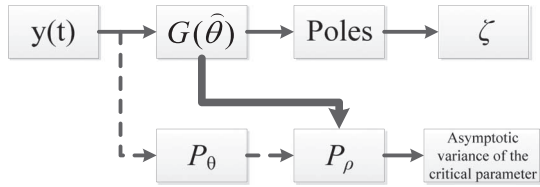

Fig. 2. Block diagram of parameter covariance matrix calculation.

around θ_0, i.e. $\sqrt{N}(\hat{\theta}-\theta_0) \sim \mathcal{N}(0, P_\theta)$ with the covariance matrix P_θ given by [16]:

$$P_\theta = \sigma_e^2 E\left[\psi(t,\hat{\theta})\psi(t,\hat{\theta})^T\right]^{-1}, \tag{3}$$

where $\psi(t,\hat{\theta}) = -(d\varepsilon(t,\theta)/d\theta)|_{\theta=\hat{\theta}}$, and σ_e^2 is a driving noise from (2). P_θ can be estimated during the identification process as follows[2] [16], [17]:

$$P_\theta = \frac{1}{N}\sum_{t=1}^{N}\varepsilon^2(t,\hat{\theta})\left(\frac{1}{N}\sum_{t=1}^{N}\psi(t,\hat{\theta})\psi(t,\hat{\theta})^T\right)^{-1}. \tag{4}$$

P_θ is a measure of the asymptotic modeling error between $G_i(\hat{\theta})$ and G_{0i} and therefore, indirectly, of the estimation error of the critical damping ratio that is deduced from $G_i(\hat{\theta})$[3]. Since P_θ is an indirect measure, it is more useful to deduce the covariance matrix P_ζ of the damping ratio estimates ($\hat{\zeta}$). Moreover, diagonal elements of P_ζ provide a quantitative measure of how accurate damping ratio estimates can be obtained using the particular signal (diagonal elements of P_ζ represent variances of the damping ratio estimates).

Suppose now that the covariance matrix P_ζ can be estimated, and that it is estimated for all measured signals y_i. The best signal for damping ratio estimation is the one that has the smallest variance of the critical damping ratio estimate (which is the corresponding element of P_ζ). This reasoning provides the basis to develop a formal algorithm for the selection of the optimal signal for mode estimation applications, which is illustrated in Fig. 1.

The sequel provides an algorithm for computation of P_ζ that uses *only ARMA model parameters* and not the dataset that is used for the identification of the ARMA model. This property makes the signal selection algorithm independent of the identification method used to determine the ARMA model.

III. Computation of the Asymptotic Parameter Covariance Matrix P_ζ

A. Theoretic Derivation

As presented in [16], [17], one way to compute the covariance matrix P_ρ of the model parameter vector $\hat{\rho}$ (one sub-vector of $\hat{\rho}$ is the vector $\hat{\zeta}$, consequently P_ζ can be extracted from P_ρ) is to use a first order Taylor approximation of the mapping between $\hat{\theta}$ and $\hat{\rho}$ (i.e. $\rho = f(\theta)$), and to project the covariance matrix P_θ (estimated using (4)), as follows:

$$P_\rho = \left(\frac{d\rho(\theta)}{d\theta}\right) P_\theta \left(\frac{d\rho(\theta)}{d\theta}\right)^T\Bigg|_{\theta=\hat{\theta}}. \tag{5}$$

However, this closed-form expression $\rho = f(\theta)$ does not exist and the matrix $d\rho(\theta)/d\theta|_{\theta=\hat{\theta}}$ must be evaluated numerically as shown in [17]. In addition, this approach assumes that P_θ is known, which means that P_θ has to be computed during the ARMA model identification (usually computed using (4)). This can be seen as a disadvantage in the case that the used identification method does not provide matrix P_θ as an output (e.g. subspace identification methods).

This paper presents an approach that computes P_ρ directly from the estimated model, and at the same time, avoids the numerical evaluation of $d\rho(\theta)/d\theta|_{\theta=\hat{\theta}}$. A block diagram of the proposed approach is illustrated in Fig. 2. (thick line), whereas the method from [17] is marked by a dashed line.

In the proposed procedure to compute P_ζ it is assumed that the ARMA model obtained is an exact representation of reality i.e. $\hat{\theta} = \theta_0$. The identified ARMA model $G_i(\theta_0)$ is reparameterized with another parameter vector ρ_0 which has the same dimension as θ_0 and whose one sub-vector is ζ_0. This allows deriving an expression for the covariance matrix P_ρ. The variance of the mode of the interest is then the corresponding diagonal element of P_ρ. The reparameterization procedure is given in the Appendix. The expression for calculation of the covariance matrix P_ρ is given in Theorem 1.

Theorem 1: Let the true SISO system G_0 be proper, monic and has a stable inverse. Also, assume that G_0 can be described by an ARMA model structure $G(\theta)$ with the parameter set θ, i.e. $\exists\theta = \theta_0$ such that $G(\theta_0) = G_0$ and that the estimate of θ_0 (denoted by $\hat{\theta}$) determined by an identification method is an accurate estimate of θ_0, i.e. it can be assumed that $\hat{\theta} = \theta_0$. Also, assume that $G(\theta)$ can be expressed in terms of another set of parameters ρ. Further, suppose that the mapping between θ and ρ is such that $\rho(\theta_0) = \rho_0$ and that $d\rho(\theta)/d\theta|_{\theta=\theta_0}$ is invertible. Then, the approximated expression for the covariance matrix of the new parameter vector P_ρ can be computed as follows:

$$P_\rho = E\left[\psi_\rho(t)\psi_\rho(t)^T\right]^{-1}, \tag{6}$$

where $\psi_\rho(t)$ is defined as:

$$\psi_p(t) = \left(\frac{dG_i(\rho)}{d\rho}\right)^T\Bigg|_{\rho=\rho_0}\left(G^{-1}(\rho_0)\right)^T e(t). \tag{7}$$

Signal $e(t)$ denotes white noise process with unity variance.

[2]Note that P_θ does not depend on the number of data samples N, however, the real variance of the estimate reduces proportionally when Nincreases.

[3]This damping ratio can be deduced by converting the discrete-time model $G_i(\hat{\theta})$ into a continuous-time model and perform a pole/zero-decomposition of this continuous transfer function.

The proof of the theorem is given in the Appendix. It is to be noted that expression (7) does not require a closed-form expression of the mapping $\rho = f(\theta)$ between θ and ρ, nor its derivatives. It only requires to be able to obtain an expression of the transfer function $G(\rho)$ and then to obtain the derivative $dG(\rho)/d\rho|_{\rho=\hat{\rho}}$ on this new expression. Even though this theorem is used here to evaluate the variance of the damping ratio, this theorem in fact is general and can be applied to other cases where a change of parameterization is necessary.

At this point it is possible to provide explanation of why traditional PMU placement algorithms are not able to find optimal PMU location for mode estimation. It was shown that the variance of the damping ratio depends only on the underlying ARMA model. However, this ARMA model is determined by two factors. The first one is a power system model and the second one is excitation (noise) that excites the system (see (2)). Therefore, PMU placement methods that use only power system models without including characteristics of the ambient excitation (which is the common case) are not able to provide a complete answer about optimal PMU placement for mode estimation applications. The importance of the excitation is also discussed in [8].

In the previous derivation, it is assumed that the order of the ARMA model is appropriately selected. This means, on the one hand, that the model order has to be high enough to describe the dynamics of the system accurately, but on the other hand, it is important to keep the order (and consequently the number of estimated parameters) as low as possible. More information about methods for optimal model order selection can be found in [18].

B. Calculation of the Parameter Covariance Matrix

This paragraph presents a numerically efficient algorithm for the computation of the asymptotic parameter covariance matrix P_ρ that is defined in Theorem 1. The term $\psi_\rho(t)$, that is given by (7), represents an output of a single-input multiple-output system that can be written in a state space form described by A, B, C, D matrices and state vector $x(t)$ as:

$$\begin{aligned} x(t+1) &= Ax(t) + Be(t) \\ \psi_\rho(t) &= Cx(t) + De(t). \end{aligned} \tag{8}$$

Using the property that $e(t)$ and $x(t)$ are independent ($E[e(t)x(t)] = 0$) and the assumption of unity variance of the white noise, the inverse of covariance matrix can be written in terms of the output state space equation:

$$\begin{aligned} E\left[\psi_\rho(t)\psi_\rho^T(t)\right] &= E\left[\left(Cx(t) + De(t)\right)\left(Cx(t) + De(t)\right)^T\right] \\ &= E\left[Cx(t)x^T(t)C^T\right] + E\left[De(t)e^T(t)D^T\right] \\ &= CX(t)C^T + DD^T \end{aligned} \tag{9}$$

where $X(t) = E[x(t)x^T(t)]$. This term can be computed from the state space (8):

$$\begin{aligned} X(t+1) &= E\left[\left(Ax(t) + Be(t)\right)\left(Ax(t) + Be(t)\right)^T\right] \\ &= E\left[Ax(t)x^T(t)A^T\right] + E\left[Be(t)e^T(t)B^T\right] \\ &= AX(t)A^T + BB^T. \end{aligned} \tag{10}$$

In steady state, asymptotically, the following equation holds $X(t+1) = X(t)$, that leads to:

$$X(t) = AX(t)A^T + BB^T, \tag{11}$$

which is a Lyapunov equation whose unknown is $X(t)$ and, that can be readily solved using e.g. MATLAB[4]. Substituting the computed $X(t)$ into (9), the value $E[\psi_\rho(t)\psi_\rho^T(t)]$ is obtained. Further, by computing the inverse of $E[\psi_\rho(t)\psi_\rho^T(t)]$ the covariance matrix P_ρ is obtained.

The previous results lead to the algorithm for computation of the parameter covariance matrix:

- Step 1) Find the parameters θ_0 of the underlying ARMA model $G_i(\theta)$ for the selected signal i using a system identification technique.
- Step 2) Express the ARMA model $G_i(\theta)$ in terms of parameters ρ to obtain $G_i(\rho)$, and find the corresponding parameters ρ_0 (see the Appendix).
- Step 3) Compute the derivatives of $G_i(\rho)$ with respect to the model parameters ρ evaluated at $\rho = \rho_0$.
- Step 4) Compute the vector of transfer functions $F = (dG_i(\rho)/d\rho)^T|_{\rho=\rho_0}(G_i^{-1}(\rho_0))^T$.
- Step 5) Express the transfer functions F in state space form with one input and a number of outputs that is equal to the number of parameters. Corresponding system matrices are denoted by A, B, C, D.
- Step 6) Solve the Lyapunov equation $A = AXA^T + BB^T$ for X.
- Step 7) Compute $E[\psi_\rho(t)\psi_\rho^T(t)] = CXC^T + BB^T$.
- Step 8) Compute the parameter covariance matrix as: $P_\rho = E[\psi_\rho(t)\psi_\rho^T(t)]^{-1}$

This procedure provides the asymptotic covariance matrix P_ρ as a final result that contains asymptotic variances of the estimated damping ratios as diagonal elements. It is important to note that values of the asymptotic variances do not depend on the number of samples used in the identification. This is not the case for absolute variance observed that linearly decrease when the longer data set is used for identification i.e. the following holds: $Cov(\sqrt{N}\hat{\theta}\rho) \to P_\rho$, as $N \to \infty$, and consequently $Cov(\hat{\theta}\rho) \to (1/N)P_\rho$.

C. Mode Estimation in Case of Multiple Critical Modes in the System

The proposed algorithm answers the question of the optimal signal selection for one critical mode of interest. If multiple modes are monitored in real-time, it is obviously possible to determine a different signal ranking for each of the critical modes (the proposed procedure is performed for each critical mode separately). Based on these results, the recommended practice for real-time mode estimation is to perform estimation separately (as parallel processes) for each critical mode using the corresponding optimal signals.

An alternative to this approach is to use an integral ranking criterion that combines the computed variances of different modes of interest (weighing sum for instance). The integral criterion provides a unique signal ranking that takes different

[4]In the MATLAB environment, this matrix equation can be solved efficiently using the function `dlyap`.

critical modes into consideration, meaning that there is no need to run parallel mode estimations (as in the previous approach). However, this ranking provides only suboptimal results (each particular mode will be estimated using suboptimal signals).

D. Remarks on Signal Selection for Mode Shape Estimation

In the analysis of electromechanical oscillations, it is also useful to obtain information about mode shapes of the critical modes [2], [19]. The sequel of this subsection provides a short discussion about important considerations for signal selection for mode shape estimation and the relationship between damping ratio and mode shape signal selection.

In contrast to damping ratio estimation, mode shape estimation does not estimate a parameter that is common for all measured signals. Rather, each location has its own true parameter value that needs to be estimated. Furthermore, it can be said that the most relevant signals are those that have the largest influence on the critical mode. Therefore, there are two aspects in signal selection for mode shapes:

1) Signals that have the largest participation in the oscillation.
2) Signals that provide the best accuracy of the mode shape estimate.

Relative mode shape that corresponds to the k-th signal is estimated as [19]:

$$M_k(\lambda_i) \approx \left.\frac{Y_k(s)}{Y_{ref}(s)}\right|_{s=\lambda_i \approx j\omega_i}, \tag{12}$$

where λ_i is a critical mode, and $Y_k(s)$ and $Y_{ref}(s)$ are Laplace Transforms of k-th and reference signals, respectively. If a white noise signal is selected as a reference signal, the mode shape estimation is reduced to ARMA model estimation. Furthermore, the signals that have a large value of such defined mode shape will also have a large participation in the oscillation, which corresponds to the first aspect of the signal selection for mode shape estimation (large signal participation).

Once the ARMA model (12) and its parameter covariance matrix P_θ are estimated, (5) can be used to obtain uncertainty of the frequency response at the mode frequency following the procedure from Section III (with the difference that in Section III the uncertainty of damping ratio estimate is obtained instead). Further, this uncertainty represents the uncertainty of the mode shape estimate and consequently a measure of accuracy that can be obtained with a particular signal (the second aspect of signal selection for mode shape estimation). Note that the new parameterization in (5) is required, i.e. $\rho(\omega) = M_k(\theta)$.

Based on these results (mode shape values and accuracy of the estimates), it is possible to make a decision on which signals should be used for mode shape estimation.

Mode shape estimation using the considerations above is beyond the scope of this manuscript, and subject to on-going research. Therefore, this will not be analyzed in more details in the sequel.

IV. Signal Selection for On-Line Application

This section first discusses the relationship between the estimated damping ratio and its variance computed by (6), and further formulates a signal pre-selection method that is beneficial for on-line applications, where computational time can be critical.

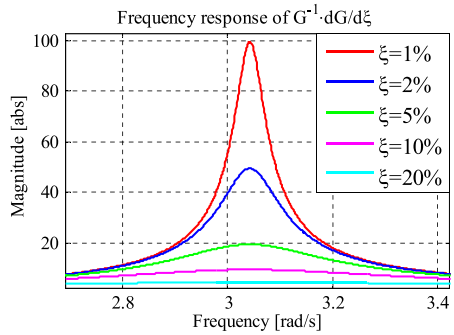

Fig. 3. Bode plot of the transfer function $F = (dG(\zeta)/d\zeta)|_{\zeta=\zeta_0} G_0^{-1}$ for different values of ζ.

A. Qualitative Analysis of the Relationship Between Damping Ratio and its Variance

To establish a qualitative relationship between damping ratio and its variance, (6) is expressed in the frequency domain by applying Parseval's theorem:

$$P_\rho = \left[\frac{1}{2\pi}\int_{-\pi}^{\pi} \frac{1}{|G_{oi}|^2}\left(\frac{dG(\rho,\omega)}{d\rho}\right)^*\Big|_{\rho=\rho_0} \times \left(\frac{dG(\rho,\omega)}{d\rho}\right)\Big|_{\rho=\rho_0} d\omega\right]^{-1}. \tag{13}$$

Using the property of the derived parameterization $G(\rho)$ that it is a product of modes' factors (see the Appendix), it is apparent that the value of the term $(1/G_{oi})(dG(\rho,\omega)/d\rho_i)|_{\rho=\rho_0}$ in depends only on the mode whose parameter is ρ_i (ρ_i is the i-th element of ρ). This is due to cancellations between G_{0i} and $dG(\rho,\omega)/d\rho_i$ for all other modes' factors. Now, it is possible to plot the frequency response of the term $[1/G_{oi}](dG(\rho,\omega)/d\rho_i)|_{\rho=\rho_0}$ for different values of ρ_i, where ρ_i represents the damping ratio of the critical mode (ζ_i) while the frequency of the mode ω_i is fixed on the value ω_{0i}. This plot is shown in Fig. 3. Note that the fixing the value of ω_i is a justified assumption since it is known that the estimate of ω_i is generally very accurate[5]. This means that the shape of the frequency response plotted in Fig. 3 does not change significantly when ω_i is changed.

It can be seen from (13) that the diagonal elements of P_ρ^{-1} are equal to the integral of the squared frequency response from Fig. 3. Now, assume that the parameter estimates $\hat{\rho}$ are mutually independent. This assumption is equal to the assumption that off-diagonal elements of the matrix P_ρ (i.e. covariances) are equal to zero[6]. Using this assumption, it can be said that

[5]This assumption does not affect generality of the approach; it only enables simplification of the reasoning and the presentation.

[6]This assumption is not fully satisfied in reality, however it enables a qualitative analysis of the relationship between the values of the parameter estimates and the signal spectrum by simplifying the computation of the matrix inverse in (11).

the value of integral in (13) is a diagonal matrix whose inverse is obtained simply by replacing the elements by their reciprocals. This means that variance of ζ_i is inversely proportional to the area below the corresponding lines in Fig. 3, which again inversely depends on ζ_i. Therefore, this directly correlates the value of the critical damping ratio ζ_i and its variance (the smaller damping ratio implies smaller variance).

This conclusion can also be derived from another approach. Let us assume that all parameters in ρ_0 except ζ_i are known and that only ζ_i has to be estimated. Using the same reasoning from (13) and Fig. 3, it follows that the larger damping ratio implies the larger estimation variance.

A critical situation in the real-life operation is when damping ratio of the critical mode decreases with time. The previous results show that, in this situation, the accuracy of the estimate will improve, which is a desirable property. On the other hand, when the damping ratio increases, the accuracy of the estimate will decrease. However, since this is not a critical situation for the grid, the smaller accuracy will not affect operation of the system.

B. Signal Pre-Selection

Running the formal algorithm described in Section III for all available synchrophasor signals in real-time can be computationally demanding. Also, this is unnecessary because the majority of the signals will contain little or no information about the mode of interest. This phenomenon might happen due to (near) zero-pole cancellation effect. For that reason, it is beneficial to develop a fast pre-selection method that will aid in determining if the signal can be considered as a candidate for optimal for mode estimation.

This pre-selection algorithm will be formulated in similar manner as the formal algorithm: A criterion that can be computed efficiently is defined and used for ranking of the signals. Using this ranking, a limited number of the top ranked signals will be selected as candidates for the optimal signal (first stage). In the second stage, the full formal algorithm from Section III will be applied on the selected signal candidates in order to determine the final ranking.

The proposed pre-selection ranking criterion is defined as the average amplitude of the signal's Fourier transform over a small range around the critical frequency. This procedure finds if there is a peak in the signal's spectrum, which indicates that the critical mode is visible in the analyzed signal. Since the value of the peak is not directly proportional to the accuracy of the obtained estimate, it is necessary to run the formal algorithm and determine the final signals' ranking for optimal mode estimation. This pre-selection criterion can be computed efficiently by using Goertzel's algorithm [20].

If a signal, due to (near) pole-zero cancellation, contains little information about the critical mode, its power spectrum will generally not have a pronounced resonance peak at the frequency of the considered mode i.e. the damping ratio of the estimated mode (if it is observable) will have a large value. Using the results from Section IV-A, it implies that the computed ranking criterion will numerically have a large value causing the signal to be discarded. This means that the bias (caused by the lack of information about the critical mode in the signal) will not affect selection of the top ranked signals.

It is important to note that this section, besides formulating the pre-selection method for signal selection, provides new insight to the commonly accepted premise that signals whose spectrum has a large peak at the mode frequency are likely to be a good choice for mode estimation [9], [10].

V. Application

In order to illustrate application of the presented methodology, the KTH Nordic 32 [21] and the IEEE test systems with 10 generators and 39 buses are used. The KTH Nordic 32 test system has one critical inter-area mode at approximately 0.5 Hz (or 3 rad/s) with damping ratio of 3.52%, which is closely studied in [21], [22]. The IEEE test system has a critical mode at 0.58 Hz with damping ratio equal to 2.29%. The simulated synchrophasor measurements are obtained from the simulations where active and reactive powers of all loads are modeled as a white noise, which is the only disturbance in the system.

A. Critical Parameter Variance Computation and Validation

The variance of the estimated damping ratio of the critical mode is computed using the methodology presented in Section III. Using methodology from [18], a model order 12 is selected as appropriate and used for all the signals. The ranking criterion (variance of the estimate) is computed assuming a first order approximation of the prediction error criterion with respect to the model parameters (see Section III and [16]) as well as Tustin approximation used for mapping between discrete and continuous domains (see Appendix). These approximations inevitably introduce errors in the computed damping ratio variance (it will deviate from the actual variance). To assess effect of these errors, the computed variance is compared with the sample variance that is obtained using the results of 2000 simulated Monte Carlo mode estimations (for each mode estimation, an independent realization of the excitation is used). This sample variance is multiplied by the number of samples used for the estimation. Modes are estimated using the prediction error method that minimizes prediction error criterion (defined in Section II) over the set of ARMA model parameters as shown in Fig. 2. In these simulations, 3000 data samples with 5 Hz sampling frequency (10 min data block) are used for each simulation. The variance obtained using Monte Carlo simulations is denoted as “observed” in the sequel.

The results obtained with the KTH Nordic 32 test system are given in Figs. 4 and 5, whereas the on-line diagram of the system with the locations of the signal candidates is presented in Fig. 6.

The results confirm that the variances computed using the approach proposed in this paper do not significantly differ from the variances obtained using Monte Carlo simulations (the difference is always less than 25%). Further, the results suggest that the voltage angle signals, if chosen carefully, provide the smallest estimation variance. However, in this particular case, it is possible to choose among a large number of voltage magnitude signals that provide reasonably good accuracy (around 0.2). Locations of the signal candidates provide further insight in the obtained results (Fig. 6).

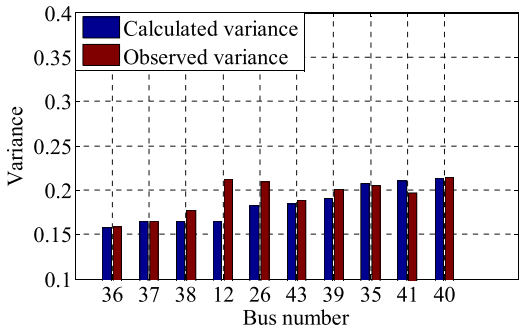

Fig. 4. Calculated and observed variance of the estimated damping ratio of the critical mode 0.5 Hz using voltage magnitude synchrophasor signals.

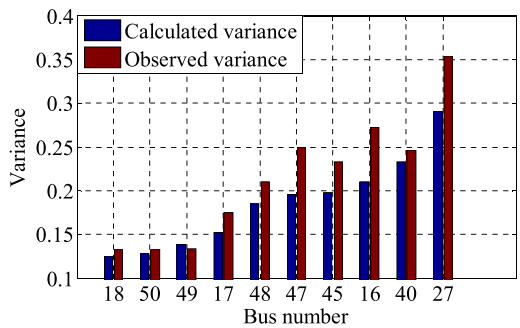

Fig. 5. Calculated and observed variance of the estimated damping ratio of the critical mode 0.5 Hz using voltage angles synchrophasor signals.

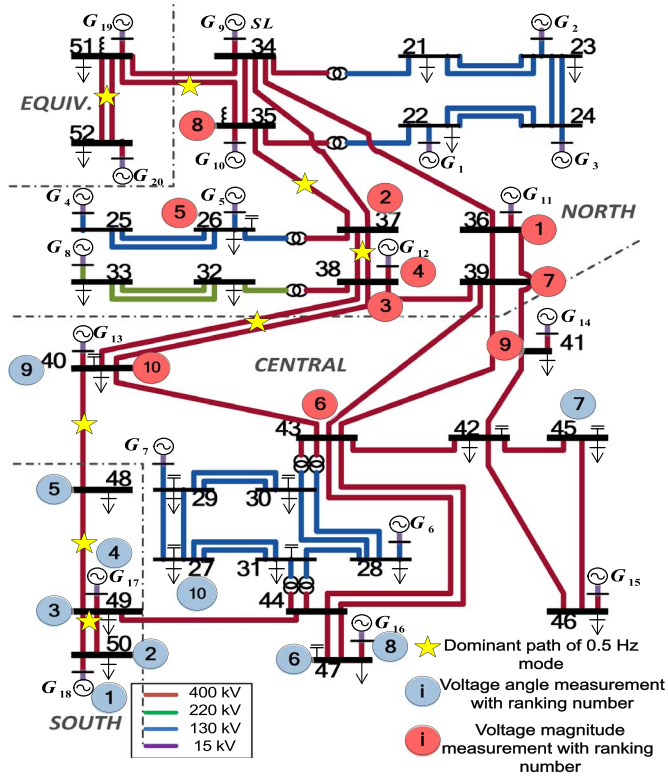

Fig. 6. Single-line diagram of the KTH Nordic 32 Test System with locations of the candidate signals for ambient mode estimation.

Note, that the obtained variances have a physical interpretation. Namely, the absolute variance when N samples are used, is simply obtained by dividing the asymptotic variance with N. Further, the absolute variance can be expressed through standard deviation. For instance, if $N = 3000$ (as used in the presented test cases), the asymptotic variance of 0.15, will represent the absolute variance of $5 \cdot 10^{-5}$, i.e. standard deviation of the damping ratio estimate is 0.707% whereas the true damping ratio value is 3.52%.

Based on the results of modal analysis it is known that the critical 0.5 Hz mode causes oscillation of the area represented by generators 17 and 18 against the Northern part of the system. It can be noticed that the best voltage angle signals are in vicinity of these generators. On the other hand, voltage magnitude signals that are in vicinity of buses 36–37 provide the smallest variance of the damping ratio. The results conclusively show that the optimal locations are very different when different signal types are used. This can be explained by the fact that voltage angles deviations will be largest in the proximity of the dominant oscillating generators, whereas voltage magnitude oscillations at these buses can be significantly suppressed by reaction of automatic voltage regulators. More details on this phenomenon can be found in [22].

The proposed algorithm has been derived with the assumption that the prediction error estimator is unbiased as commonly assumed in mode estimation algorithms. However, due to the zero pole cancelation and the reduced model order that is used to describe the full system dynamics, a certain amount of bias is an inevitable consequence. This bias is a complex phenomenon for which an analytical expression does not exist. In the sequel,

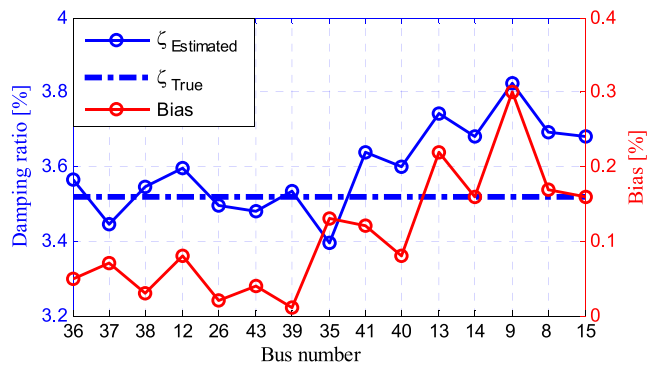

Fig. 7. Bias analysis of the top ranked voltage magnitude signals from the KTH Nordic 32 test system.

the bias obtained with different signals is analyzed using Monte Carlo simulations. For each signal, 2000 Monte Carlo mode simulations are run and the mean value of the mode damping ratio estimates is used for the bias calculation (the bias is a difference between this value and the true value which is equal to 3.52%).

Figs. 7 and 8 show damping ratio estimates obtained as a mean of the 2000 estimates from Monte Carlo simulations, as well as the absolute value of the bias (the red line shows the absolute value of the difference between the solid blue line and the true damping ratio value denoted by the blue dashed-dotted line). Fig. 7 shows results for 15 top-ranked voltage magnitude signals, whereas Fig. 8 shows results for 15 top-ranked voltage angle signals.

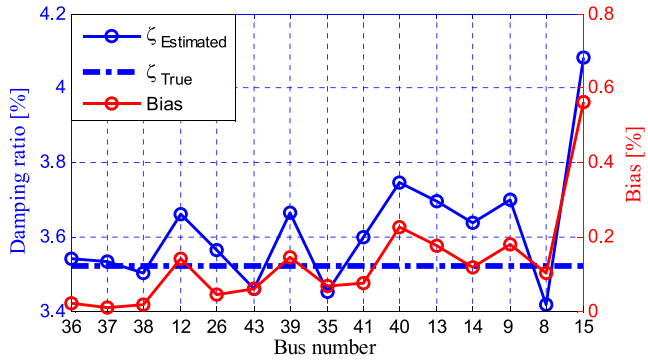

Fig. 8. Bias analysis of the top ranked voltage angle signals from the KTH Nordic 32 test system.

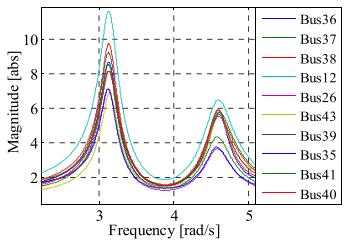

Fig. 9. Power spectra of the best ten voltage magnitude signals ranked based on the methodology from Section III.

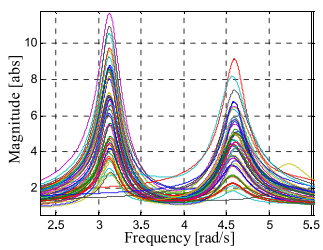

Fig. 10. Power spectra of all of the voltage magnitude signals.

The results suggest that the top ranked signals with the proposed methods tend to provide a smaller value of the bias (the red lines in Figs. 7 and 8 are almost monotonically increasing).

B. Signal Pre-Selection

As it was concluded in Section IV, power spectrums of the measured signals can be used for optimal signal pre-selection. In other words, the optimal signals for damping ratio estimation will have large peaks in their spectra at the critical mode frequency. The validity of this assumption is analyzed by comparing power spectrums of the voltage magnitude signals. The results are presented in Figs. 9 and 10.

Figs. 9 and 10 show that the ten best signals for the 0.5 Hz mode have in general large peaks (according to Fig. 9) comparing to the all signals whose power spectra are given in Fig. 10.

Numerical comparisons between the pre-selection and formal algorithm for voltage magnitude signals are given in Table I.

It can be seen that among the first ten signals that are determined by the pre-selection algorithm, the 4 best signals computed by the formal algorithm are present. Also, the best ten signals determined by the formal algorithm (highlighted) are contained in the 22 first signals computed by the pre-selection algorithm. Further, it can be noticed that pre-selection tends to favor the signals measured directly at the middle voltage generator buses (buses denoted by numbers 1–20) even though these signals do not ensure the optimal mode estimation (according to the formal algorithm).

A similar analysis has been conducted for voltage angle signals, and the results are reported in Table II.

Table II shows even better matching between the pre-selection and formal algorithm in case of voltage angle signals, comparing to the voltage magnitude signals. The first 15 pre-selected signals contain ten best signals determined by the formal algorithm.

TABLE I
COMPARISON OF THE PRE-SELECTION AND FORMAL ALGORITHM IN THE CASE OF VOLTAGE MAGNITUDE SIGNALS

	Pre-selection		Proposed method	
	Bus No.	Criterion Value	Bus No.	Criterion Value
1	**12**	11.61	**36**	0.160
2	14	10.88	**37**	0.164
3	11	10.46	**38**	0.164
4	**38**	9.73	**12**	0.164
5	13	9.54	**26**	0.182
6	**39**	9.20	**43**	0.184
7	15	8.75	**39**	0.191
8	**36**	8.66	**35**	0.201
9	5	8.63	**41**	0.210
10	**37**	8.48	**40**	0.213
11	9	8.47	13	0.221
12	32	8.46	14	0.228
13	10	8.32	9	0.231
14	**40**	8.16	8	0.239
15	**41**	8.14	15	0.242
16	8	7.98	11	0.251
17	34	7.21	1	0.253
18	**26**	7.09	22	0.261
19	**35**	7.06	34	0.262
20	1	7.04	24	0.271
21	42	7.02	45	0.285
22	**43**	6.90	25	0.298

TABLE II
COMPARISON OF THE PRE-SELECTION AND FORMAL ALGORITHM IN THE CASE OF VOLTAGE ANGLE SIGNALS

	Pre-selection		Proposed method	
	Bus No.	Criterion Value	Bus No.	Criterion Value
1	**16**	21.66	**18**	0.125
2	**18**	21.43	**50**	0.129
3	**50**	20.35	**49**	0.139
4	**49**	19.74	**17**	0.153
5	**48**	19.01	**48**	0.185
6	**47**	15.83	**47**	0.196
7	**17**	12.90	**45**	0.198
8	**45**	12.63	**16**	0.210
9	7	10.79	**40**	0.233
10	46	10.62	**27**	0.291
11	29	7.19	46	0.316
12	**27**	7.15	13	0.324
13	31	7.10	43	0.349
14	41	6.81	16	0.354
15	**40**	6.62	29	0.372

TABLE III
COMPARISON OF DIFFERENT SIGNAL SELECTION ALGORITHMS USING VOLTAGE MAGNITUDE SIGNALS FROM THE KTH NORDIC 32 TEST SYSTEM

Observed variance (Bus /Value)		Proposed method (Bus / Value)		CF1[9] (Bus / Value)		MPC[8] (Bus / Value)	
36	0.155	36	0.16	42	0.453	40	27.98
37	0.167	37	0.164	37	0.150	47	26.82
38	0.172	38	0.164	39	0.143	42	4.16
43	0.180	12	0.164	14	0.113	38	3.73
39	0.198	18	0.182	15	0.104	51	2.75
40	0.203	43	0.184	51	0.098	14	2.29
41	0.205	39	0.191	31	0.090	31	1.64
35	0.206	35	0.201	34	0.081	25	1.53
26	0.209	41	0.21	36	0.079	16	1.51
12	0.207	40	0.213	6	0.079	52	1.47

TABLE IV
COMPARISON OF DIFFERENT SIGNAL SELECTION ALGORITHMS USING VOLTAGE ANGLES SIGNALS FROM THE KTH NORDIC 32 TEST SYSTEM

Observed variance (Bus /Value)		Proposed method (Bus / Value)		CF1[9] (Bus / Value)		MPC[8] (Bus / Value)	
18	0.131	18	0.125	18	0.169	6	2.76
50	0.133	50	0.129	7	0.161	17	1.81
49	0.134	49	0.139	29	0.146	7	1.66
44	0.159	17	0.153	16	0.129	13	1.13
17	0.171	48	0.185	31	0.129	18	0.82
28	0.191	47	0.196	17	0.126	40	0.74
48	0.209	45	0.198	6	0.115	16	0.65
45	0.232	16	0.210	51	0.092	47	0.49
40	0.241	40	0.233	40	0.088	31	0.46
47	0.252	27	0.291	50	0.076	44	0.421

C. Comparison of Signal Selection Methods

This section provides comparison among different signal selection methods, namely the proposed method is compared with the methods proposed in [9] (denoted by CF1) and in [8] (denoted by MPC). In addition, variance of the damping ratio estimate obtained using Monte Carlo simulations is reported (observed variance), even though this method is not applicable for on-line signal selection.

First, voltage magnitude and angle signals synthetized using the KTH Nordic 32 test system were used to obtain rankings with different criteria. The values of different computed criteria and corresponding rankings (top ten signals for each criterion) are shown in Tables III and IV.

The results show that the final ranking results obtained with different algorithms differ significantly, however it can still be noticed from Fig. 6 that buses selected with different methods are relatively close to each other with some exceptions.

Figs. 11 and 12 show performances of the three signal selection methods in terms of the obtained bias that is calculated using 2000 Monte Carlo simulations. The results are shown for the top ten ranked signals (as in Tables III and IV) separately for voltage magnitude (Fig. 11) and voltage angle (Fig. 12) signals.

The presented results show that the top ranked signals with the proposed method provide smaller values of bias (with a few exceptions). This can be seen from the fact that the blue line is placed below other lines for most signals.

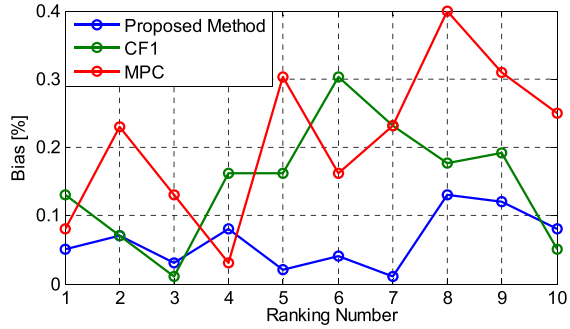

Fig. 11. Comparison of biases obtained with the top-ranked voltage magnitude signals from the KTH Nordic 32 test system using different signal selection methods.

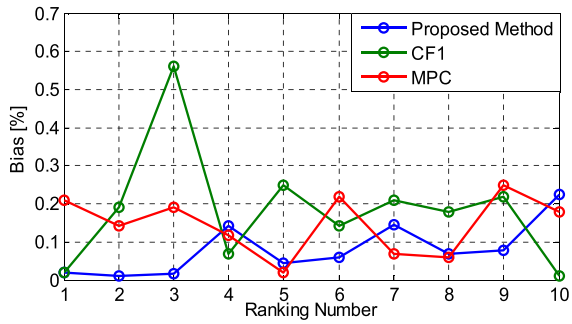

Fig. 12. Comparison of biases obtained with the top-ranked voltage angle signals from the KTH Nordic 32 test system using different signal selection methods.

Further, this comparison is performed using the IEEE Test system with 39 buses and ten generators. Characteristic of this system is that it has one critical mode at 0.58 Hz and damping ratio of 2.29%, where generator 1 has a very large inertia, which makes other generators oscillate against generator 1. A single-line diagram of the test system with optimal locations determined by the proposed method is shown in Fig. 13.

Numerical results obtained by the different signal selection methods are presented in Tables V and VI. These results suggest that the optimal locations for voltage angle signals are closer to the generators than the voltage magnitude signals. A difficulty with this system is that there is no single dominant mode path, rather, there are multiple paths that transfer oscillations from generator 1 to other oscillating generators. This explains relatively dispersed optimal locations.

The results obtained using the other two methods ([8] and [9]) show that the 10 top optimal locations overlap to the some extent with the results from the proposed method. Due to multiple mode paths this system in general shows that several locations can provide sufficiently good mode estimation results.

Similarly to Figs. 11 and 12, bias analysis is performed for IEEE 39 bus system. The results are shown in Figs. 14 and 15 where a similar conclusion can be drawn, which is that the proposed method generally selects signals that also provide smaller bias.

D. Effect of Measurement Noise and Selected Model Order on the Calculated Ranking Criterion

Presence of measurement noise alters the spectrum of the measured signal and, consequently, the mode estimation

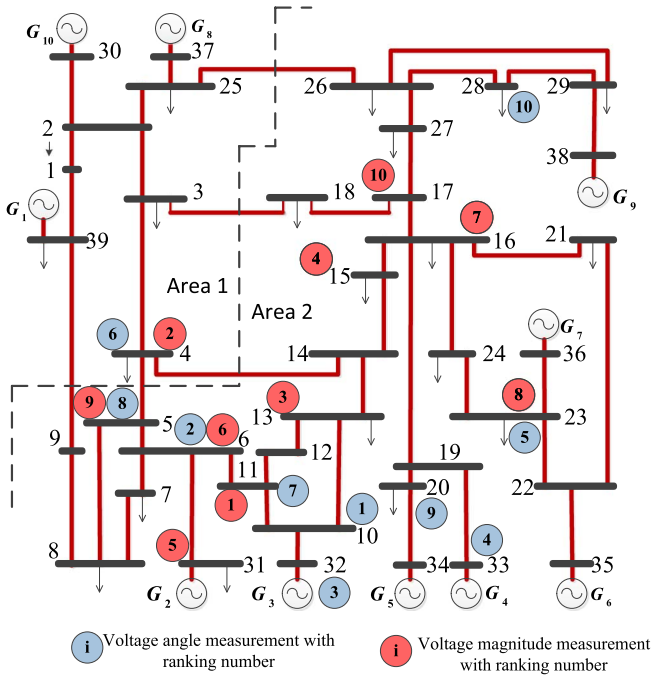

Fig. 13. Single-line diagram of the KTH Nordic 32 Test System with locations of the candidate signals for ambient mode estimation.

TABLE V
COMPARISON OF DIFFERENT SIGNAL SELECTION ALGORITHMS USING VOLTAGE MAGNITUDE SIGNALS FROM THE IEEE 39-BUS TEST SYSTEM

Observed variance (Bus /Value)		Proposed method (Bus / Value)		CF1[9] (Bus / Value)		MPC[8] (Bus / Value)	
13	0.158	11	0.122	16	0.156	28	1.228
11	0.172	4	0.122	11	0.123	31	0.792
12	0.184	13	0.124	33	0.101	34	0.783
31	0.161	15	0.141	25	0.099	15	0.740
32	0.183	31	0.152	12	0.083	32	0.739
15	0.192	6	0.161	31	0.081	29	0.693
27	0.208	16	0.162	13	0.069	10	0.690
10	0.210	23	0.175	23	0.068	8	0.635
14	0.216	5	0.181	5	0.064	33	0.623
6	0.222	17	0.193	27	0.062	16	0.622

TABLE VI
COMPARISON OF DIFFERENT SIGNAL SELECTION ALGORITHMS USING VOLTAGE ANGLES SIGNALS FROM THE IEEE 39-BUS TEST SYSTEM

Observed variance (Bus /Value)		Proposed method (Bus / Value)		CF1 [9] (Bus / Value)		MPC [8] (Bus / Value)	
11	0.051	10	0.049	16	0.156	33	1.14
4	0.053	6	0.049	11	0.123	32	1.11
6	0.054	32	0.050	33	0.101	31	0.75
23	0.056	33	0.050	29	0.091	20	0.51
28	0.057	23	0.051	12	0.083	23	0.43
12	0.059	4	0.053	26	0.072	26	0.35
26	0.064	11	0.053	10	0.071	15	0.30
10	0.069	5	0.054	23	0.068	6	0.29
5	0.070	20	0.056	6	0.063	10	0.28
32	0.073	28	0.056	28	0.057	5	0.27

results and estimated variance of the damping ratio. Effects of measurement noise on mode estimation is analyzed in

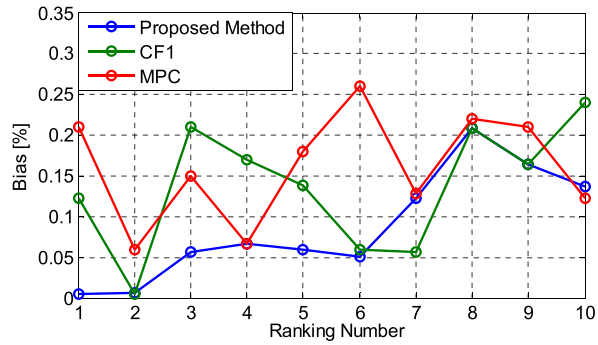

Fig. 14. Comparison of biases obtained with the top-ranked voltage magnitude signals from the IEEE 39-bus test system using different signal selection methods.

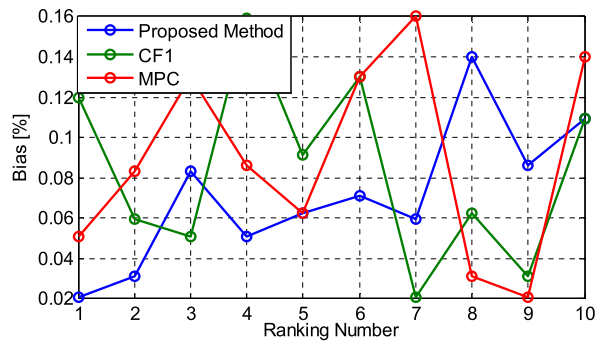

Fig. 15. Comparison of biases obtained with the top-ranked voltage angles signals from the IEEE 39-bus test system using different signal selection methods.

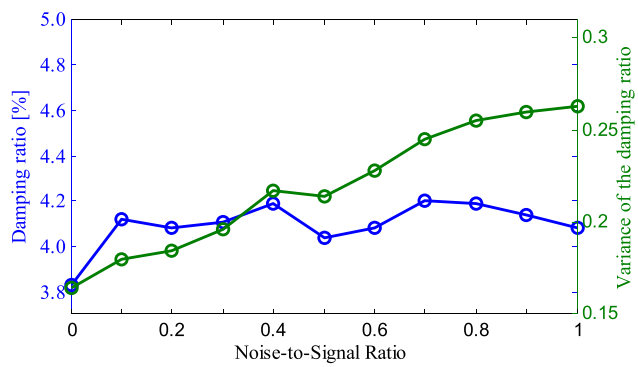

Fig. 16. Effect of measurement noise on computed ranking criterion.

[14], [23], whereas effect on the estimated damping variance (ranking criterion) is analyzed in the sequel. This is done by analyzing signals that are synthetized by adding different levels of white Gaussian noise [described by noise-to-signal power ratio (NSR)] to the voltage magnitude signal of bus 38 (the KTH Nordic 32 test system). The synthetized signals are used for ARMA model estimation with settings described in the previous section. Finally, the obtained ARMA models are used as an input to the proposed method to obtain variances of the critical damping ratio. The results of the performed analyses show (Fig. 16) how the estimated critical damping ratio and its variance change with different level of noise.

The results show that the measurement noise increases the estimated variance. The final ranking of the signals will obviously depend on level of the noise on each measurement, however a

TABLE VII
EFFECTS OF THE SELECTED MODEL ORDER ON THE ESTIMATED VARIANCE OF THE CRITICAL MODE'S DAMPING RATIO

Model order	Voltage magnitude		Voltage angles	
	Bus 38	Bus 36	Bus 18	Bus 49
10	0.232	0.178	0.126	0.112
11	0.155	0.152	0.125	0.133
12	**0.161**	**0.153**	**0.124**	**0.134**
13	0.165	0.168	0.134	0.125
14	0.153	0.161	0.121	0.144
15	0.154	0.158	0.129	0.136
16	0.160	0.168	0.120	0.152

positive thing is that signals with more noise will be negatively penalized (the computed variance increases with noise).

In the previous studies, model of the ARMA model was selected to be equal to 12 (determined using methodologies from [18]). However, it is necessary to assess how results of the proposed methodology change when sub-optimal model order is selected. To do that, the KTH Nordic 32 test system is used to simulate one realization of synchrophasor signals. These signals are used as an input to the proposed method where different values of the selected ARMA model orders are used. The calculated damping ratio variances (criterion values) for different signals are shown in Table VII.

Table VII shows that the computed variance does not change significantly when model order is non-optimal, but even this small deviation can cause change in the final signal ranking. However, it has to be noted that as long as the model order is high enough to describe the dynamics of the system and if a real-time mode estimator uses the same model order, the obtained ranking will be correct even when non-optimal order is used (the mode estimation will not be optimal but because the estimated variance is correct, the ranking will be adequate).

E. Computational Performance of the Proposed Method

Following the description of the proposed algorithm in Section III, it is possible to assess its computational performance. The first step of the proposed algorithm is pre-selection. A typical required time for the pre-selection ranking criterion (FFT analysis) computation using a MATLAB implementation and an off-the-shelf personal computer (Intel i7, 2.7 GHz CPU, 8 GB of RAM) is around 0.4 ms per signal.

The result of the pre-selection method is a list of a relatively small number of signals (less than 50 regardless of the system size) for which the final ranking criterion has to be computed. The final ranking criterion for one signal is computed as follows:

1) *ARMA model computation* (Step 1 in Section III-B). Formally, this is not part of the ranking criterion computation. ARMA models can be obtained from different sources. For instance, following the two level architecture from [11], ARMA models can be computed at the substation level.
2) *Model manipulation* (Steps 2–5 from Section III-B).
3) *Variance calculation* (Steps 6–8 from Section III-B).

Typical required computational times for the above procedures using a MATLAB implementation a personal computer are given in Table VIII.

TABLE VIII
COMPUTATIONAL PERFORMANCES OF THE PROPOSED SIGNAL SELECTION METHOD

Model order	ARMA computation	Model manipulation	Variance calculation
10	1.441 s	0.175 s	0.018 s
12	1.841 s	0.258 s	0.023 s
14	1.916 s	0.341 s	0.027 s
16	2.049 s	0.465 s	0.031 s

The results show that total computational time, even for the largest systems can be held below 60 s (30 pre-selected signals, 2 s each), whereas the criterion computation time itself can be held below 10 s. By applying the decentralized approach proposed in [10], [11] or using a compiled programming language with better performances (C for example), the computational time can be significantly reduced. Regardless, this time delay is acceptable, especially taking into account that a long data blocks (10 minutes in the presented case studies) are used as an input, which makes a 60 s delay relatively small.

VI. CONCLUSION

This paper proposed a criterion and an algorithm that ranks synchrophasor signals according to their ability to estimate parameters of the critical mode (frequencies and damping ratios) with lowest variance. The value of the ranking criterion is computed directly from the model that describes spectrum of the measured synchrophasor signal. These models can be obtained in two ways depending on the application: 1) from the physical model of the power system in the case of off-line PMU placement problem with the objective of optimal mode estimation, or 2) from on-line measurements in the case of on-line optimal signal selection problem which is used for mode estimation.

This paper emphasizes the fact that mode estimation, as one of the most important synchrophasor applications, requires special attention, even in the planning stage when PMU locations are decided. Traditionally, this was not the case because PMU locations are mainly determined based on state estimation application requirements. Also, during the operation it is advisable to periodically check if the used signals provide the best possible results because operational changes in the power system can cause a change in the critical modes as well as the signals that contain the most information about these modes.

APPENDIX

A. Derivation of the Parameterization Suitable for Mode Estimation Application

For the mode estimation application, accurate estimation of the mode damping ratios (ζ) are of essential importance. This means that a new parameterization is required where these parameters (ζ) are in the vector of model parameters ρ. To do this, the identified transfer function is expressed in terms of discrete poles and zeros and then transformed to the continuous domain using the well-known Tustin approximation. Once, the poles/zeros are expressed as continuous variables, they can be written in terms of frequencies and damping ratios. The parameterization obtained contains the parameters of interest (ζ) in

the vector of parameters (ρ). This procedure is demonstrated in the sequel.

The estimated ARMA model in terms of discrete zeros, poles and gain can be written as follows:

$$H_{(z)}=k\frac{\prod\limits_{\substack{i\in Real\\ Zeros}}(1-q_{ri}z^{-1})\prod\limits_{\substack{i\in Cplx\\ Zeros}}(1-q_{ci}z^{-1})\left(1-q_{ci}^{*}z^{-1}\right)}{\prod\limits_{\substack{i\in Real\\ Poles}}(1-p_{ri}z^{-1})\prod\limits_{\substack{i\in Cplx\\ Poles}}(1-p_{ci}z^{-1})\left(1-p_{ci}^{*}z^{-1}\right)}. \tag{A1}$$

To express poles/zeros frequencies and damping ratios, the discrete poles and zeros have to be substituted by continuous domain poles and zeros. This is done by using Tustin's approximation (A2) that gives the relationship between discrete and continuous domains [24]:

$$t_i=\frac{1+0.5c_iT_s}{1-0.5c_iT_s}, \tag{A2}$$

where $t_i\in\{q_{ci},p_{ci}\}$ and c_i is the i-th continuous domain pole/zero (calculated in advance). The real continuous domain poles/zeros do not need to be expressed in terms of continuous domain poles/zeros because there is no frequency and damping ratio associated to these poles/zeros. In the case of complex poles/zeros, the expression (A2) has to be expressed in terms of pole/zero frequency and damping ratio using the following relationship:

$$c_i=-\xi_i\omega_i\pm\omega_i\sqrt{\zeta_i^2-1}, \tag{A3}$$

where ζ_i is damping ratio of i-th pole/zero and ω_i its natural frequency. By substituting (A3) into (A2), the following is obtained:

$$t_i=\frac{1\mp\frac{1}{2}\zeta_i\omega_iT_s\pm\frac{1}{2}\omega_iT_s\sqrt{\zeta_i^2-1}}{1\pm\frac{1}{2}\zeta_i\omega_iT_s\mp\frac{1}{2}\omega_iT_s\sqrt{\zeta_i^2-1}}. \tag{A4}$$

Expression (A4) represents the relationship between the desired parameterization (ρ) and known discrete poles/zeros. Finally, by substituting (A4) into (A1), the reparameterized model is obtained whose derivatives can be easily calculated (that is needed for solving (6)). One factor of the reparameterized model is shown in (A5)–(A7) (other factors have a similar form):

$$\left(1-t_iz^{-1}\right)\left(1-t_i^{*}z^{-1}\right)=1-2\mathrm{Re}\{t_i\}z^{-1}+|t_i|^2z^{-2} \tag{A5}$$

The real part and amplitude of t_i are as follows:

$$\mathrm{Re}\{t_i\}=\frac{1-0.25\omega_i^2T_s^2}{1+\xi_i\omega_iT_s+0.25\omega_i^2T_s^2}, \tag{A6}$$

$$|t_i|^2=\frac{\left(1-0.25\omega_i^2T_s^2\right)^2+\left(1-\xi_i^2\right)\omega_i^2T_s^2}{\left(1+\xi_i\omega_iT_s+0.25\omega_i^2T_s^2\right)^2}. \tag{A7}$$

At this point, derivatives of the factors of $H(\rho)$ can be easily computed, i.e. transfer function $(dG(\rho)/d\rho)^T|_{\rho=\rho_0}$ from (7) can be determined. It can be noted that only the derivatives of elementary factors have to be computed because the remaining transfer function does not depend on the parameters of the corresponding elementary factor (other factors are constant).

B. Proof of Theorem 1

Without losing generality, it can assumed in (3) that the variance of the driving noise σ_e^2 is equal to one because P_θ does not depend on σ_e^2. Also, note that the following equation holds: $(dG_i(\theta)/d\theta)^T|_{\theta=\theta_0} = (dG_i(\rho)/d\rho)(d\rho(\theta)/d\theta)_{\theta=\theta_0\vee\rho=f(\theta_0)\rho_0}$, (assuming that ρ is a function of θ, i.e. $\rho=f(\theta)$). Using this expression and the relationship $\psi(t,\theta)=-d\varepsilon(\theta)/d\theta=G_{0i}^{-1}[(dG_i(\theta))/d\theta]e(t)$, $\psi(t,\theta)$ can be written as:

$$\begin{aligned}\psi(t,0)&=\left(G_{0i}^{-1}\frac{dG_i(\rho)}{d\rho}\frac{d\rho(\theta)}{d\theta}\right)^T\Bigg|_{\theta=\theta_0\wedge\rho=f(\theta_0)=\rho_0}e(t)\\&=\left(\frac{d\rho(\theta)}{d\theta}\right)^T\left(\frac{dG_i(\rho)}{d\rho}\right)^T\Bigg|_{\theta=\theta_0\wedge\rho=f(\theta_0)=\rho_0}\\&\quad\times\left(G_{0i}^{-1}\right)^Te(t)\\&=\left(\frac{d\rho(\theta)}{d\theta}\right)^T\Bigg|_{\theta=\theta_0}\psi_\rho(t);\end{aligned} \tag{B1}$$

where the following notation is used:

$$\psi_\rho(t,\rho)=\left(\frac{dG_i(\rho)}{d\rho}\right)^T\Bigg|_{\rho=\rho_0}\left(G_{0i}^{-1}\right)^Te(t). \tag{B2}$$

Substituting this expression in (3) results in:

$$P_\theta^{-1}=\left(\frac{d\rho(\theta)}{d\theta}\right)^TE\left[\psi_\rho(t)\psi_\rho^T(t)\right]\left(\frac{d\rho(\theta)}{d\theta}\right)\Bigg|_{\theta=\theta_0}; \tag{B3}$$

where the fact that $(d\rho(\theta)/d\theta)|_{\theta=\theta_0}$ is a deterministic matrix is used. To simplify notation, this can be written as:

$$P_\theta^{-1}=\left(\frac{d\rho(\theta)}{d\theta}\right)^TP_\rho^{-1}\frac{d\rho(\theta)}{d\theta}\Bigg|_{\theta=\theta_0}, \tag{B4}$$

where $P_\rho^{-1}=E[\psi_\rho(t)\psi_\rho^T(t)]$ as defined in the Theorem 1.

Taking an inversion of the (B4) and replacing θ_0 by its estimate $\hat{\theta}$, the expression (5) is obtained, i.e.:

$$P_\rho=\left(\frac{d\rho(\theta)}{d\theta}\right)P_\theta\left(\frac{d\rho(\theta)}{d\theta}\right)^T\Bigg|_{\theta=\hat{\theta}} \tag{B5}$$

This concludes the proof of the theorem.

REFERENCES

[1] F. Galvan and P. Overholt, "The intelligent grid enters a new dimension," *Transm. Distrib. World*, vol. 66, no. 8, pp. 22–29, Jul. 2014.

[2] , J. J. Sanchez-Gasca, Ed., "Identification of electromechanical modes in power systems," in *IEEE Task Force Report*. : Special Publication TP462, 2012.

[3] , A. Messina, Ed., *Inter-Area Oscillations in Power Systems: A Nonlinear and Nonstationary Perspective*. New York, NY, USA: Springer-Verlag, 2009.

[4] L. Dosiek and J. W. Pierre, "Estimating electromechanical modes and mode shapes using the multichannel ARMAX model," *IEEE Trans Power Syst.*, vol. 28, no. 2, pp. 1950–1959, May 2013.

[5] G. Liu and V. M. Venkatasubramanian, "Oscillation monitoring from ambient PMU measurements by Frequency Domain Decomposition," in *Proc. IEEE Int. Symp. Circuits Syst.*, May 18–21, 2008, pp. 2821–2824.

[6] S. A. N. Sarmadi and V. M. Venkatasubramanian, "Electromechanical mode estimation using recursive adaptive stochastic subspace identification," *IEEE Trans. Power Syst.*, vol. 29, no. 1, pp. 349–358, Jan. 2014.
[7] [Online]. Available: www.naspi.org
[8] D. J. Vowles and M. J. Gibbard, "Illustration of an analytical method for selecting signals and locations for power system modal-estimators," in *Proc. . IEEE PES General Meeting*, Jul. 25–29, 2010, pp. 1–7.
[9] J. Zhang, C. Wu, and Y. Han, "A power spectrum density based signal selection approach for electromechanical mode estimation," in *Proc. IEEE PES General Meeting*, Jul. 22–26, 2012, pp. 1–7.
[10] J. Ning, X. Pan, and V. M. Venkatasubramanian, "Oscillation modal analysis from ambient synchrophasor data using distributed frequency domain optimization," *IEEE Trans. Power Syst.*, vol. 28, no. 2, pp. 2556–2566, May 2013.
[11] J. Ning, S. A. N Sarmadi, and V. M. Venkatasubramanian, "Two-level ambient oscillation modal estimation from synchrophasor measurements," *IEEE Trans. Power Syst.*, vol. 30, no. 6, pp. 2913–2922, Nov. 2015.
[12] M. Dehghani, B. Shayanfard, and A. R. Khayatian, "PMU ranking based on singular value decomposition of dynamic stability matrix," *IEEE Trans. Power Syst.*, vol. 28, no. 3, pp. 2263–2270, Aug. 2013.
[13] S. Ranjana, S. C. Srivastava, and S. N. Singh, "Optimal PMU placement method for complete topological and numerical observability of power system," *Electr. Power Syst. Res.*, vol. 80, no. 9, pp. 1154–1159, Sep. 2010.
[14] V. S. Perić and L. Vanfretti, "Power-system ambient-mode estimation considering spectral load properties," *IEEE Trans. Power Syst.*, vol. 29, no. 3, pp. 1133–1143, May 2014.
[15] N. Jacobsen, P. Andersen, and R. Brincker, "Applications of frequency domain curve-fitting in the EFDD technique," in *Proc. IMAC-XXVI: Conf. & Expo. on Structural Dynamics*, Feb. 4–7, 2008, pp. 1–13.
[16] L. Ljung, *System identification theory for the user*. Englewood Cliffs, NJ, USA: Prentice-Hall, 1999.
[17] H. Ghasemi and C. A. Canizares, "Confidence intervals estimation in the identification of electromechanical modes from ambient noise," *IEEE Trans. Power Syst.*, vol. 23, no. 2, pp. 641–648, May 2008.
[18] V. S. Perić, T. Bogodorova, A. N. Mete, and L. Vanfretti, "Model order selection for probing-based power system mode estimation," in *Proc. Power and Energy Conf. at Illinois*, Feb, 20–21, 2015, pp. 1–5.
[19] N. Zhou, Z. Huang, L. Dosiek, D Trudnowski, and J. W. Pierre, "Electromechanical mode shape estimation based on transfer function identification using PMU measurements," in *Proc. IEEE PES General Meeting 2009*, Jul. 26–30, 2009, pp. 1–7.
[20] C. Park and S. Ko, "The hopping discrete Fourier transform," *IEEE Signal Process. Mag.*, vol. 31, no. 2, pp. 135–139, Mar. 2014.
[21] Y. Chompoobutrgool, W. Li, and L. Vanfretti, "Development and implementation of a Nordic grid model for power system small-signal and transient stability studies in a free and open source software," in *Proc. IEEE PES General Meeting*, Jul. 22–26, 2012, pp. 1–8.
[22] Y. Chompoobutrgool and L. Vanfretti, "Identification of power system dominant inter-area oscillation paths," *IEEE Trans. Power Syst.*, vol. 28, no. 3, pp. 2798–2807, Aug. 2013.
[23] J. Turunen *et al.*, "Comparison of three electromechanical oscillation damping estimation methods," *IEEE Trans. Power Syst.*, vol. 26, no. 4, pp. 2398–2407, Nov. 2011.
[24] A. V. Oppenheim and R. W. Schafer, *Discrete-time signal processing*, Third ed. Upper Saddle River, NJ, USA: Prentice-Hall, 2009.

Vedran S. Perić (S'12) received the M.S. degree in power systems and M.S. degree in power electronics from the University of Novi Sad, Serbia. He is currently working toward the Ph.D. degree at the Department of Electric Power Systems, KTH Royal Institute of Technology, Stockholm, Sweden.

From 2008 to 2011, he was a Research and Teaching Assistant with the University of Novi Sad. From October 2013 through July 2014, he was a Visiting Researcher with the Delft University of Technology, Delft, The Netherlands. His research interests include power system operation and control, and application of phasor measurement units in stability assessment and enhancement.

Xavier Bombois was born in Brussels in 1974. He received the Electrical Engineering and Ph.D. degrees from the Université Catholique de Louvain, Louvain-la-Neuve, Belgium, in 1997 and 2000, respectively.

After his Ph.D. dissertation, he joined the Delft University of Technology, Delft, The Netherlands, where he was appointed an Assistant Professor with the Delft Center for Systems and Control in 2001. Since February 2015, he has been a CNRS Research Director with Laboratoire Ampère, Ecole Centrale de Lyon, Ecully, France. His main interests are identification for control, prediction error identification, optimal experiment design, uncertainty bounding and robust control.

Mr. Bombois is an associate editor for the IFAC journal *Control Engineering Practice* and for the Conference Editorial Board of the IEEE Control Systems Society.

Luigi Vanfretti (S'03–M'10–SM'13) received the Electrical Engineering degree from Universidad de San Carlos de Guatemala, Guatemala City, Guatemala, in 2005, and the M.Sc. and Ph.D. degrees in electric power engineering from Rensselaer Polytechnic Institute, Troy, NY, USA, in 2007 and 2009, respectively.

He was a Visiting Researcher with The University of Glasgow, Glasgow, Scotland, in 2005. He became an Assistant Professor with the KTH Royal Institute of Technology, Stockholm, Sweden, in 2010 and was conferred the Swedish title of "Docent" in 2012, and obtained a tenured Associate Professor position in 2013. He is the Principal Investigator at KTH for the FP7 EU projects iTesla and IDE4L, and for the NER-funded project STRONg^{2}rid. He is currently a Special Advisor in R&D Strategy and International Collaboration for the Research and Development Division of Statnett SF, the Norwegian transmission system operator; where he has previously held positions as Special Advisor in Strategy during 2013–2014, and as external scientific advisor during 2011–2012. He is an advocate and evangelist for free/libre and open-source software. His research interests are in the general area of power system dynamics, while his main focus is on the development of applications of PMU data.

Dr. Vanfretti, has served, since 2009, in the IEEE Power Engineering Society (PES) PSDP Working Group on Power System Dynamic Measurements, becoming Chair in 2014. In addition, from 2009 to 2014, he served as Vice-Chair of the IEEE PES CAMS Task Force on Open Source Software. For his research and teaching work toward his Ph.D. degree, he was awarded the Charles M. Close Award from Rensselaer Polytechnic Institute.